Selenium isotope analysis by N-TIMS: Potential and challenges

Hauke Vollstaedt[1,2,*], Klaus Mezger[1,2], Thomas Nägler[1], Ingo Leya[2,3], and Anne Trinquier[4]

[1]Institute of Geological Sciences, University of Bern, Baltzerstrasse 1+3, 3012 Bern, Switzerland

[2]Center for Space and Habitability, University of Bern, Sidlerstrasse 5, 3012 Bern, Switzerland

[3]Institute of Physics, University of Bern, Sidlerstrasse 5, 3012 Bern, Switzerland

[4]Thermo Fisher Scientific, Hanna-Kunath-Str. 11, 28199 Bremen, Germany

[*]Corresponding author (hauke.vollstaedt@geo.unibe.ch)

Keywords: TIMS; N-TIMS; selenium; isotopes; double spike

Abstract

The isotope composition of selenium (Se) can provide important constraints on biological, geochemical, and cosmochemical processes taking place in different reservoirs on Earth and during planet formation. To provide precise qualitative and quantitative information on these processes, accurate and highly precise isotope data need to be obtained. The currently applied ICP-MS methods for Se isotope measurements are compromised by the necessity to perform a large number of interference corrections. Differences in these correction methods can lead to discrepancies in published Se isotope values of rock standards which are significantly higher than the acclaimed precision. An independent analytical approach applying a double spike (DS) and state-of-the-art TIMS may yield better precision due to its smaller number of interferences and could test the accuracy of data obtained by ICP-MS approaches. This study shows that the precision of Se isotope measurements performed with two different Thermo Scientific™ Triton™ Plus TIMS is distinctly deteriorated by about ±1 ‰ (2 s.d.) due to $\delta^{80/78}$Se by a memory Se signal of up to several millivolts and additional minor residual mass bias which could not be corrected for with the common isotope fractionation laws. This memory Se has a variable isotope composition with a DS fraction of up to 20 % and accumulates with increasing number of measurements. Thus it represents an accumulation of Se from previous Se measurements with a potential addition from a sample or machine blank. Several cleaning techniques of the MS parts were tried to decrease the memory signal, but were not sufficient to perform precise Se isotope analysis. If these serious memory problems can be overcome in the future, the precision and accuracy of Se isotope analysis with TIMS should be significantly better than those of the current ICP-MS approaches.

1. Introduction

The abundance, isotope composition, and oxidation state of Se in environmental reservoirs is a subject of intense interest in many scientific disciplines [1]. Studies on the Se isotope composition focus on the present and past marine geochemistry [2-7], exogenic processes [8], the oxygenation of the atmosphere [9], and the biogeochemical cycling of Se [10-17]. Selenium can be found in four oxidation states in nature: +VI (selenate), +IV (selenite), 0 (elemental selenium) and -II (selenide).

Selenium isotopes are commonly measured with a hydride generation system connected to an inductively coupled plasma multicollector mass spectrometer (HG-ICP-MS). The external precision (2 s.d.) of current analytical approaches using HG-ICP-MS ranges between 0.02 and 0.14 ‰/amu (as determined by repeated analyses of the USGS SGR-1 rock standard [2-4, 17, 18]. However, a large number of isobaric interferences like Ar_2, ArCl, Ge, NiO, and hydrides formed with Ar_2, As, Ge, and Se require the application of on-peak zero corrections [19]. The details of this interference correction differ between the published studies and may be the reason for the observed discrepancies in the published Se isotope values of rock standards of up to 0.5 ‰ in $\delta^{82/76}$Se [4]. Furthermore, different ICP-MS instruments and HG systems result in different intensities of the interfering signals. Therefore, an independent analytical approach that does not require a large number of isobaric and non-isobaric corrections may lead to a better precision and could test the accuracy of data obtained by the HG-ICP-MS approaches.

Thermal ionisation mass spectrometers operating in negative ionisation mode (n-TIMS) have being used for a long time for determining Se abundances and its isotope composition with a precision of 0.05 ‰/amu (2 s.d.) [13, 20]. However, in these early studies Se isotopes had to be measured in dynamic mode because of a limited dispersion of the MS at that time. Due to recent

advances in analytical instrumentation, static mode measurements for all Se isotopes and interferences from mass 73 to 82 are now possible. This study explores the potential of Se isotope analysis with state-of-the-art TIMS.

2. Methods

Selenium isotope measurements were carried out at the Institute of Geological Sciences in Bern, Switzerland and at Thermo Fisher Scientific in Bremen, Germany using a Thermo Scientific TRITON Plus TIMS. Measurements were operated in negative ionisation mode with a 10 kV acceleration voltage and 10^{11} Ω and 10^{12} Ω resistors for the Faraday cups, depending on the signal strength. Selenium isotopes were generally measured on single Re filaments (30μm thick, 7mm wide), but double filament set-ups were found to give similar signal intensity and stability. The filaments were outgassed for 70 min at 4 A and the entrance slit of the ion source was replaced before each measurement session. All filament parts (filaments, sides, covers) and the entrance slit were physically cleaned with an abrasive non-woven medium grain size SCOTCH-BRITE®, subsequently cleaned with ethanol and purified water (18.2 MΩ) in an ultrasonic bath, and dried at 50 °C in an oven.

The highest and most stable Se isotope signals were achieved by loading and dispersing 1 μl of a saturated $Ba(OH)_2$ activator solution (~25 μg Ba), made from barium hydroxide octahydrate (> 98% purity, Sigma Aldrich), on the filament and gently drying the solution at 0.5 A. Afterwards, 500 ng Se of the SRM 3149 standard (distributed by the National Institute of Standards and Technology), which was mixed with 20 ng C from an Aquadag® graphite colloidal solution (Acheson Industries Inc.) and dried down at 80 °C on a hot plate, was taken up with 1.5 μl purified water and loaded on top of the dried $Ba(OH)_2$ solution and finally dried down at 0.5 A.

The amplifier gain was measured at the beginning of every measurement session. The measurements started with an automatically controlled exponential heating sequence, which is described in table 1. Afterwards, the standard was heated manually with 20 mA/min, interrupted by periodic focussing and peak centring, until the Se signal intensity stopped to increase. Typical ranges of final filament currents were 1350 to 1550 mA corresponding to 900 to 1050 °C, which are similar to earlier approaches [13]. For the measurements carried out in Bern, a typical run consisted 100 scans separated into ten blocks with 16.8 s integration and 3 s idle time each, leading to a total integration time of 28 minutes. Typically, the Se signal decreased within this integration time by about 50 %. The electronic baseline was recorded by deflecting the ion beam before each block.

The application of a double spike (DS) technique and iterative spike correction algorithm that uses the exponential law for the mass fractionation correction enables the determination of natural $^{80}Se/^{78}Se$-ratios. The iterative evaluation routine closely follows the one presented earlier for stable Sr isotopes [21] which is based on the classical isotope dilution equation and on a similar algorithm presented earlier for Pb isotopes [22]. We used a ^{77}Se-^{74}Se DS prepared from single isotope standards (ISOFLEX Russia, Moscow, Russian Federation) having isotope enrichments of 99.2 % and 99.96 % for ^{77}Se and ^{74}Se, respectively. The enriched material was dissolved individually in concentrated HNO_3 and then mixed gravimetrically according to the compositions suggested by the double spike toolbox [23]. The DS was calibrated by mixing the SRM 3149 standard and the DS in DS/SRM 3149 proportions from 0.5 to 1.1 of total Se, which were then used to constrain the pure spike composition (Table 2). We used the $^{77}Se/^{74}Se$, $^{78}Se/^{74}Se$, and $^{80}Se/^{74}Se$ as the DS inversion isotope ratios for calculating naturally occurring

stable isotope fractionation in $^{80}Se/^{78}Se$. The Se isotope variations, expressed as $\delta^{80/78}Se$ relative to the standard SRM 3149 single element solution, are calculated using the following relation:

$$\delta^{80/78}Se_{sample}[‰] = \left(\frac{\left({}^{80}Se/{}^{78}Se \right)_{sample}}{\left({}^{80}Se/{}^{78}Se \right)_{SRM\,3149}} - 1 \right) * 1000$$

3. Results

Over a measurement period of about 30 minutes average Se signals of ~1-2 V were observed for 500 ng Se, which is slightly higher compared to literature data for other TIMS measurements [13]. Current ICP-MS-based methods use similar to significantly less amounts of Se [4, 18]. However, the Se N-TIMS method has not yet been fully optimized and potential exists for analysis of much less than 500 ng Se. The noise on the amplifiers was determined by running a method of 10 blocks, 30 cycles, 4 s integration time, with a baseline at start and with no filament heating. The noise (2 s.d.) of the 10^{11} Ω amplifiers is 34 to 36 μV, which results in a signal to noise ratio (SNR) of higher than 4000 for the cup with the lowest signal (average ^{78}Se signal of an isotopically diluted (id) standard is about 150 mV). This SNR is similar or better than current MC-ICP-MS methods due to the required measurements of on-peak zeros of the latter method (SNR ~100 on ^{76}Se, ~1000 on ^{78}Se). Isotope measurements on n-TIMS do not suffer from isobaric interferences of Ar_2, ArCl, Ge, NiO, or hydrides formed with Ar_2, As, Ge, and Se [19]. This ultimately allows the precise measurement of ^{80}Se on TIMS (natural abundance of 49.6 % [24]), which is not possible with HG-ICP-MS methods due to large interferences from $^{40}Ar^{40}Ar$ dimers. Additional interferences from Ge are greatly reduced due to the different vaporization temperatures (~1800 °C for Ge [25] and ~1100 °C for Se). The monitored mass 73 signal was always below the detection limit showing that our standard is free of any significant amount of

Ge, which has an isobaric interference on ^{74}Se. A ~1 V signal was observed on masses 79 and 81 at temperatures of ~900 to ~1000 °C, which could be attributed to Br coming from the $Ba(OH)_2$ activator.

The first measurements were performed on unspiked (isotope composition (ic)) SRM 3149 standards to determine the analytical precision of $^{80}Se/^{78}Se$ measurements. This reference material is a single element standard solution, which is not isotopically certified and has become the isotopic reference standard of choice for Se. In a diagram of average logarithmic raw $^{80}Se/^{74}Se$ vs. $^{80}Se/^{78}Se$ block ratios ($(^{xx}Se/^{xx}Se)_{raw}$) all standards define a slope of 0.441±0.125 (2 s.d.; n = 7), which overlaps with theoretical predictions from the exponential (0.481) and power (0.500) isotope fractionation laws [26] (Figure 1A). Although the slopes of the linear regression through the average block ratios of single standard runs have a large uncertainty due to the low ^{74}Se signal of about 2 to 30 mV, they also largely overlap with the theoretical slopes defined by the mass fractionation laws (Figure 1B). Similar observations were made for other Se isotope ratios but with lower uncertainties on the slopes due to higher natural abundances. Residual trends in normalised $^{80}Se/^{78}Se$ ($^{80}Se/^{78}Se_{norm}$) remain for some standards when normalising to the naturally occurring $^{82}Se/^{78}Se$ ratio of 0.176003 [24] applying the exponential mass fractionation law. These residual trends generally occur at lower signal intensities (^{80}Se, ^{78}Se, ^{82}Se lower than 1 V, 0.46 V, and 0.18 V, respectively). The $^{80}Se/^{78}Se_{norm}$ of all ic SRM 3149 standards shown in Figure 1 have an average of 2.08958 ± 0.00107 (2 s.d., n = 7). Evaluating only cycles with $^{80}Se \geq 1V$ the average $^{80}Se/^{78}Se_{norm}$ is 2.08987 ± 0.00015 (2 s.d., n = 3 (151 cycles in total)). The precision refers to about 0.08 ‰ (2 s.d.) on the $\delta^{80/78}Se$ ratio and is better than previously published TIMS results [13]. It is noted that there are different factors contributing to the precision on $\delta^{80/78}Se$ between the method applied in this study and the method

by Johnson, Herbel, Bullen and Zawislanski [13], because in the present study the $^{80}Se/^{78}Se$ is normalised to a fixed value involving three isotopes whereas the DS inversion uses four isotopes. However, the signal intensity of the least abundant isotope is higher for the DS inversion when compared to the normalisation to a fixed value.

The measured Se isotope ratios of id SRM 3149 standards do not follow theoretical predictions from isotope fractionation laws. In a plot of logarithmic $(^{78}Se/^{74}Se)_{raw}$ and $(^{80}Se/^{78}Se)_{raw}$ ratios (Figure 2B and 2C), the slope of the linear regression through the average block ratios of the individual standards is in most cases lower than predicted, which leads to drifting normalised isotope ratios over a measurement of 30 minutes. Some samples even show non-linear trends in the $\ln(^{78}Se/^{74}Se)$-$\ln(^{80}Se/^{78}Se)$ space. The drifts and non-linear trends lead to differences in $\delta^{80/78}Se$ of up to 2 ‰ over the measurement of the same standard. Drifting normalised isotope ratios are also observed for any later measured ic SRM 3149 standard (Figure 2A; see also chapter 4.3). Further, we measured different $\delta^{80/78}Se$ for two runs at different filament currents/temperatures of the same id SRM 3149 standard and filament (Figure 3). Interestingly, the $\delta^{80/78}Se$ does not significantly change during the second run at a constant filament current at 1.34 A, although the signal intensity is decreasing by a factor of three. The difference in $\delta^{80/78}Se$ between the first run at 1.16 A and the second run of 1.34 A is 0.7 ‰.

The deviation from the mass fractionation laws leads to i) drifting normalised isotope ratios over the course of the measurement and ii) different average $\delta^{80/78}Se$ values for the same standard, even for measurements on the same filament at different temperatures. The effect on the external reproducibility of $\delta^{80/78}Se$ results is difficult to assess and different for every measurement session, but roughly in the range of ±1 ‰ (2 s.d.), i.e. one order of magnitude higher than published values by Johnson, Herbel, Bullen and Zawislanski [13]. Therefore, the precision is by

far not enough for isotope ratio studies in environmental reservoirs. Nevertheless, the reproducibility is high enough for the determination of Se concentrations by isotope dilution to a precision <5% (2 s.d.).

4. Discussion

There are several possible mechanisms leading to drifting $\delta^{80/78}$Se values over the course of a measurement. Other elements with a similar volatility as Se, like K, Rb, Pb, or Ge have been measured highly precise using TIMS, which implies that the measurement of volatile elements is not a general problem on TIMS. The deviation of machine-based isotope fractionation from theoretical predictions leads to residual trends in normalised isotope data and has been previously reported for Os, Nd, and Ca isotopes [27-30]. However, the results from the first measured ic SRM 3149 standards (Figure 1) indicate that the machine-based isotope fractionation is the same within uncertainty as predicted from theoretical laws [26]. Nevertheless, any minor differences in mass discrimination behaviour cannot be excluded, but these are not responsible for the large differences of up to 1‰ in $\delta^{80/78}$Se within single standard runs (Figure 3) and between different samples. It can also be excluded i) a constant memory Se contribution from somewhere in the ion source as this would get more dominant when the standard signal intensity decreases and/or ii) Se that is homogeneously mixed with the standard material as this would not lead to different $\delta^{80/78}$Se at different filament temperatures. The largest drifts were observed for small amounts of pure double spike which has an isotope composition farthest from the memory isotope composition (see chapter 4.2). Especially, ratios of a spike isotope to a natural isotope drift considerably, hinting towards a mixing of two or more Se components.

We also tested for changes in the gain factors and baselines which might lead to shifts in $\delta^{80/78}$Se. For this a set-up employing only 10^{11} Ω amplifier resistors was used that were sequentially connected to all Faraday cups involved in the measurement to rule out any problems in the gain calibration. In another approach the electronic baseline was measured between the peaks at half masses (analytical baseline) instead of defocusing the whole beam (electronic baseline). For both approaches shifts in $\delta^{80/78}$Se with the same magnitude were observed.

The accuracy of the spike calibration has an influence on the $\delta^{80/78}$Se of standards with different spike to sample ratios. We always spiked the standards to the same total Se DS amount of 54±5 % (gravimetric precision), thereby minimizing any effects of a possible inaccurate DS calibration. Further, the significant differences in $\delta^{80/78}$Se of 0.7‰ of the same sample at different temperatures cannot be attributed to an inaccurate DS calibration. The large differences in average normalised ratios of later measured ic standards (Figure 2A) also require an alternative explanation. We therefore conclude that an inaccurate spike calibration cannot account for the bulk of the intra- and interspecific differences in $\delta^{80/78}$Se.

However, inhomogeneous loads of the spike and standard on the filament, isobaric interferences or large electron clouds in the TIMS source may lead to drifting isotope ratios. Further, an addition of blank or memory Se is another possibility to generate drifts in normalised isotope ratios and different $\delta^{80/78}$Se of the same sample at different filament temperatures. As a consequence the standard method was modified to investigate the dependence of the magnitude of the drift in isotope ratios on the modified parameters.

4.1. Modifications of the standard method

4.1.1. Graphite solution

Graphite was found to be the most effective inhibitor for Se volatilisation at low temperatures. For the standard method we used the commercially available Aquadag® colloidal graphite solution which has a very small grain size (90 % <1 μm, max 5 μm particle size). Also tried was another graphite solution made from graphite powder (Alfa Aesar, 99.9995 % purity, 2-15 μm particle size) to investigate possible Se contaminations of these materials. Due to the coarser grain size, this graphite solution resulted in a lower Se signal of ~0.4 V but still drifting isotope ratios. Therefore using the Alfa Aesar solution has not improved the measurement of isotope ratios. The Se concentration of Aquadag®, determined by high-resolution continuum-source atomic absorption spectrometry (HR-CS AAS) with the hydride technique, was found to be less than 60 ng/g, corresponding to $<1.2\times10^{-3}$ pg loaded onto the filament. Experiments were also done with silica gel as an inhibitor for Se volatilisation, which was made following the recipe of Gerstenberger and Haase [31]. However, the total Se signal was about two times lower than for graphite and normalised isotope ratios were still drifting during the course of the measurement.

4.1.2. Activator

We tried different $Ba(OH)_2$ activator solutions for the enhancement of Se ionisation and for investigating possible Se blank contributions. The solutions were prepared from barium oxide or barium hydroxide octahydrate. However, barium hydroxide is known to produce large amounts of electrons within the ion source which might have an effect on the electric potential of the ion source lenses and therefore might influence the ion beam. Therefore, a $Ba(OH)_2$-NaOH mixture was also tested as an activator and prepared following the recipe of Birck, Barman and Capmas

231 [32]. This loading solution produces fewer electrons in the source. However, not only
232 significantly lower Se intensities were obtained but still drifting isotope ratios after the
233 normalisation and a detectable Se blank when loading a filament only with Aquadag® and the
234 $Ba(OH)_2$-NaOH mixture.

235 **4.1.3. Inhomogeneous loads of spike and sample on the filament**

236 Different oxidation states of Se in an imperfect mixture of SRM 3149 and DS may be a reason
237 for drifting normalised isotope ratios of id standards during the measurements. To test for this the
238 standard-DS mixture was heated for one day at 80 °C in 14.4 M HNO_3, then dried to incipient
239 dryness, then taken up in 14.4 M HNO_3, and heated for another day at 80 °C to convert all Se to
240 the +VI oxidation state. In another test the mixture was heated for one hour at 80 °C in 6.4 M
241 HCl, which effectively converts all Se to the +IV oxidation state [33]. Both approaches did not
242 result in a reduction of the drift of normalised isotope ratios. Rather it was observed that heated
243 mixtures in HNO_3 resulted in the large drifts in normalised isotope ratios and a low
244 reproducibility in $\delta^{80/78}$Se. In another approach we varied the loading size on the filament to
245 investigate emissions of Se with different DS fractions from different spots on the filament.
246 Specifically, the activator and Se standard were distributed over 1/1, 3/4, 1/2, 1/4, 1/8 of the
247 filament. The loading size did not systematically change the results and drifts in normalised
248 isotope ratios were observed for all standards. Therefore, mixing of Se from different parts of the
249 filaments is a minor reason for the drifting isotope ratios.

250 **4.1.4. Filament heating slopes and current intensities**

251 Different final heating slopes (20mA/min, 10mA/min, and 5mA/min) were tried until reaching
252 the maximum Se signal and also different final Se signal intensities (500mV, 300mV, and

100mV on ^{80}Se). In another approach we performed an interblock heating to maintain the initial Se signal constant in a range of ±10 %. All approaches did not systematically change the precision or decreased the drift in normalised isotope ratios.

4.2. Se blank and memory

When measuring a filament only loaded with ~25 µg 98 % $Ba(OH)_2$, a total Se signal on the order of 5-10 mV is observed at the start of the measurement. The Se isotope composition was found to be variable and a mixture between natural and DS Se. The purity grade (98 %, 99.99 %, and 99.995 %) and the amount of loaded $Ba(OH)_2$ (1µl - 10µl activator solution) was found to have no influence on the Se isotope composition and the signal intensity. The background Se therefore comes from at least two distinct sources, most probably from deposited and remobilized Se in the source of the TIMS ("memory Se", having variable Se isotope composition) and with minor additions of natural Se coming from the activator ("blank Se"). Non-linear trends observed in the $\ln(^{78}Se/^{74}Se)$-$\ln(^{80}Se/^{78}Se)$ space (Figure 2) further argue for a lack of homogenisation between the blank and the standard. During about 30 minutes of measurement time the isotope ratio of the blank did not change. However, in one case an evolution of the memory Se from 4 % to 1 % spike fraction and a contemporaneous decrease in the total Se signal from ~80 mV to ~20 mV was observed for a memory Se during a measurement lasting about three days. It should be noted that this measurement was exceptionally long and had an unusually high signal whereas normally the signal lasts only for a few hours at the most.

The amount of DS in the memory Se ranges from 0 to 20 % and reflects different periods of measurements. Several approaches were tried to decrease the memory Se, including i) cleaning the filament parts with HNO_3, HCl, ethanol, and acetone, ii) using new filament parts, iii)

cleaning the TIMS source walls and the ionisation contact arm with 1M HNO_3 and ethanol, iv) cleaning the TIMS ion source by the protocol delivered by Thermo Fisher, v) cleaning the extraction slit with silicon carbide, 0.5M HNO_3, and H_2O, vi) using a new ion source, vii) baking the TIMS source (12h) and flight tube, viii) cleaning the sample wheel (either with RBS50 (Chemical Products R. Borghgraef S.A.) or a hand pad containing aluminium oxide followed by silicon carbide, 0.5M HNO_3, deionised H_2O, and ethanol), and ix) heating a blank Re filament up to 5A for several hours. None of these procedures was sufficient to either remove the memory completely or to change it to a natural Se isotope composition. However, it was found that the memory Se isotope composition changes systematically in response to some of the cleaning techniques. For one measurement the 98 % $Ba(OH)_2$ gave a Se signal of 10 mV with a DS fraction of 5 % (Figure 4). This amount of DS could be reduced to about 2 % by heating a blank Re filament to 3 A for 12 h. Further mechanical cleaning of the sample wheel and the sample chamber walls resulted in a reduction of the DS Se to about 1 % with an initial memory Se signal intensity of 2.5 mV. After measuring only 2 id standards with 500 ng Se each, the initial memory Se signal increased to ~6 mV with a DS fraction of about 20 %. Heating a blank Re filament at 5 A for one hour did not shift the blank considerably towards natural Se isotope composition. Three hours heating at 5 A shifted the memory Se composition to about 10 % DS fraction and further 14 h heating shifted the memory DS Se fraction to about 2 %. Therefore, the contribution of memory Se increases very rapidly, which would make it necessary to induce measures to reduce it after every sample by heating a Re filament to 5 A. However, this cleaning procedure was found to be not sufficient to ensure the precise determination of Se isotopes using the Triton TIMS. Furthermore, heating of a blank Re filament for >10 h is not feasible for routine Se isotope analysis. Curiously, no Se signal was detected during the heating process. Interestingly,

the maximum memory Se signal for filaments only loaded with $Ba(OH)_2$ is observed at temperatures that are about 50 – 100 °C higher than the temperature during analysis, indicating that higher temperatures are needed to remobilize Se from the TRITON Plus TIMS source parts. The deposition of elements like Sr, K, and Rb on mass spectrometer parts has been known for a long time and requires regular physical or thermal cleaning [34]. Specifically, volatile elements seem to be efficiently evaporated during the consequent sample runs. However, for Se, the cleaning techniques did not result in a sufficient removal of Se from the source parts. The deposition and later evaporation of Se from parts of the mass spectrometer has not been observed during previous Se studies on different machines. Possibly, the specific design of the Triton Plus TIMS promotes this behaviour.

4.3. Measurements at Thermo Fisher Scientific

To test our observations and hypotheses and to evaluate if these problems are specific for the system located in Bern or for all TRITON Plus TIMS, several ic and id standards, DS, and pure $Ba(OH)_2$ (98 % purity) were measured on an identically constructed machine at the Thermo Fisher Scientific factory in Bremen (Table 3). For these experiments, typically 15-30 blocks were measured each consisting of ten cycles with an integration of four seconds and three seconds idle time per cycle, leading to a total measurement time of ~18-36 minutes.

The first two ic measurements (Figure 5A) were performed before any measurement of DS containing standards. The linear fit through the average logarithmic $(^{78}Se/^{74}Se)_{raw}$ and $(^{80}Se/^{78}Se)_{raw}$ block ratios of these standards define a slope of 0.537±0.089 which overlaps with power and exponential mass fractionation laws.

The three id measurements define slopes of 0.639±0.223, 0.474±0.080, and 0.483±0.091 for sequence numbers 5, 12, and 13 respectively and therefore all coincide with the mass fractionation laws. The small, but insignificant, deviation of the slope average from the exponential mass fractionation law leads to much smaller remaining drifts in $\delta^{80/78}$Se ranging from 0.002-0.26 ‰ over a measurement period of 18 minutes. Nevertheless, slight changes in $\delta^{80/78}$Se were also noticed during large changes in signal intensity or filament temperature, which might be related to variable admixtures of a memory Se with a different isotope composition.

Any ic standard measured after the three id measurements shows a parallel shift relative to the linear regression, which corresponds to an addition of 0.005-0.05 % DS of Se (Figure 5A). These shifts towards the DS isotope composition also become visible for the ic measurement with the highest DS admixture (sequence number 14) when plotting the $\ln(^{78}Se/^{77}Se)_{raw}$ ratio on the x-axis. However, the difference in $^{78}Se/^{77}Se$ between natural Se and the DS Se is only a factor of ~2000 while it is ~20000 for the $^{78}Se/^{74}Se$. The concordant shift in $^{78}Se/^{74}Se$ and $^{78}Se/^{77}Se$ further argues against an interference-related shift of isotope ratios. The DS fraction of the $Ba(OH)_2$ activator measurements was found to be variable and range from 8 to 70 % with maximum signal intensities between 0.03 and 0.18 mV (measured on the secondary electron multiplier (SEM)). Considering the DS fractions of the $Ba(OH)_2$ measured directly before the respective ic standard, the DS admixtures in the ic standards correspond to about 0.1-0.5 mV total Se signal, which is in the same range as the signal intensities measured on filament loaded only with $Ba(OH)_2$. The Se signal intensity of the $Ba(OH)_2$ measurements in Bremen is about one order of magnitude lower than for the measurements in Bern, most probably due to the fewer standard runs on this machine.

4.4. Correction methods

Accepting that the Se blank within the ion source could not be removed efficiently for routine Se isotope analysis, the isotope composition of the blank could potentially be used to correct drifting isotope ratios for all analyses from the same sample wheel. The slope of logarithmically plotted average id isotope ratios of the ten blocks is consistently shifted from theoretical predictions to lower values (Figure 2C). Actually, subtracting a constant signal with the memory Se isotope composition leads to steeper slopes in a $\ln(^{80}Se/^{78}Se)_{raw}$ vs. $\ln(^{78}Se/^{74}Se)_{raw}$ plot, but memory Se signals of more than 100 mV are needed to obtain a slope of -0.5, which were never measured. Higher calculated memory Se signals during sample measurements when compared to pure $Ba(OH)_2$ may indicate that evaporation of memory Se from the source parts is promoted by Se emitted from the filament. However, the subtraction correction did not return slopes of -0.5 for all of the samples, probably because of a change of Se isotope composition and signal intensity of the blank during the course of a measurement (see chapter 4.2). This correction method therefore did not lead to more accurate and precise Se isotope data.

4.5 Model calculations

To assess the impact of the Se memory on the final $\delta^{80/78}Se$ data of samples and standards model calculations for a theoretical dataset were done. Specifically, an id sample was mixed with a memory Se signal, both having defined spike fractions and fractionation factors β. The fractionation factor β is calculated with the following relation:

$$\beta = \frac{\log\left(\frac{\left({}^{80}Se/{}^{78}Se\right)_{std}}{\left({}^{80}Se/{}^{78}Se\right)_{meas}}\right)}{\log\left(\frac{M_{80}}{M_{78}}\right)}$$

Where M is the mass of the respective isotope. For the standard model a total Se sample signal was assumed that is linearly decreasing during the course of the measurement from 1 V to 0.5 V within 150 cycles. The DS fraction of the sample ($f_{DS\text{-}sample}$) is set to 54 %, according to the compositions suggested by the double spike toolbox [23]. The value β_{sample} is linearly decreasing from 0 to -0.5 during the course of the measurement, a value that is typically observed for the first measured ic samples on the two different TIMS instruments used in this study (Fig. 1 and Fig. 5). A β of -0.5 is equal to about 13‰ difference in $\delta^{80/78}$Se. The sample signal is mixed with a constant memory signal of 10 mV, i.e. 1 – 2 % of the total Se signal (f_{memory}), having a DS fraction ($f_{DS\text{-}memory}$) of 5 %. The isotope composition of the memory is expected to be light, because it represents isotopically light Se emitted from the filament that is deposited in the TIMS. The remobilisation of the memory will also favour the light isotopes to be enriched in the admixing gas phase. Accordingly, a constant β_{memory} of 1.0 was chosen for the standard model. Note that an identical fractionation factor of the memory and the sample will not lead to any changes in the $\delta^{80/78}$Se irrespective of differences in f_{memory}, $f_{DS\text{-}memory}$ and $f_{DS\text{-}sample}$. Due to the admixture of 1 % - 2 % memory, the $\Delta^{80/78}$Se (defined as the difference in $\delta^{80/78}$Se relative to the first cycle of the standard model) decreases from 0 ‰ to – 0.48‰ in the standard model. To evaluate the impact of the several parameters on the $\Delta^{80/78}$Se a sensitivity study was performed. In different scenarios the β_{memory} was modified to constant values of 0.0, 0.5, 2.0, and to linearly increase from 1.0 to 2.0 in another scenario (Fig. 6A). The change in β_{memory} leads to variations of about 1-2‰ in the $\Delta^{80/78}$Se within and between different model scenarios and is therefore a very sensitive parameter. The f_{memory} was modified to constant values of 5 mV and 20 mV (0.5 % - 1.0 % and 2.0 % - 4.0 % of the total Se signal) which influenced the final $\Delta^{80/78}$Se by up to 1.5 ‰ for samples with different memory admixtures (Fig. 6B). We measured $f_{DS\text{-}memory}$ between

1 % and 20 % in the memory (Fig. 4) and these values were found to change the $\Delta^{80/78}$Se slightly by about 0.3‰ between different model scenarios (Fig. 6C). The $f_{DS\text{-}sample}$ was varied between 41 % and 68% and changed the final $\Delta^{80/78}$Se by up to 0.6‰ between model runs with different DS amounts (Fig. 6D). Note that an identical f_{DS} of the sample and the memory will lead to a drift of only 0.01‰ in the course of the standard run. The β_{sample} does not influence the final $\Delta^{80/78}$Se as it is cancelled out by the DS algorithm. The general observation from the sensitivity study is that the more different the sample and the memory are in terms of fractionation and DS amounts, the higher the impact is on the finally calculated $\Delta^{80/78}$Se. Accordingly, measuring samples with similar f_{DS} will likely reduce drifting of isotope ratios as the memory will have a similar f_{DS} to the sample. The combined effects of β_{memory}, f_{memory}, $f_{DS\text{-}memory}$, and $f_{DS\text{-}sample}$ are in the same order as the estimated external reproducibility of ±1 ‰ and are therefore able to account for the observed variations in the measured $\delta^{80/78}$Se.

5. Conclusions

Negative-TIMS analysis with state-of-the-art mass spectrometers carries the potential to decrease the number of isobaric interferences for Se isotope measurements and to increase the precision significantly compared to the currently applied HG-ICP-MS approaches. During the course of this study it was possible to obtain total average Se signals of about 1-2 V over a measurement period of about 30 minutes for about 500 ng of Se. In contrast to a previous TIMS approach [13] all Se isotopes and interference masses could be measured in static operational mode. However, normalised Se isotope ratios drifted over the course of the measurements leading to a poor $\delta^{80/78}$Se reproducibility of about ±1 ‰, which is more than one order of magnitude higher

compared to the currently achieved precision with HG-ICP-MS. The drifts in $\delta^{80/78}$Se are caused by a Se memory emitted from parts of the ion source in the MS and potentially additional minor residual mass bias which could not be corrected for with the common isotope fractionation laws. The memory Se isotope composition was found to be variable and to be a mixture of natural and DS Se, implying that it was introduced into the machine during the measurements. The memory Se accumulates with the number of measured standards and reached several mV in signal. Model calculations suggest that about 1 % admixture of an isotopically fractionated Se memory is able to account for the in-run drifts and differences between different samples of about 1-2 ‰ in $\delta^{80/78}$Se. The observations of a Se memory were made on two different mass spectrometers of the same type. Applying different cleaning techniques to the mass spectrometer source, sample wheel, and filament parts decreased the blank amount in parts but not down levels sufficient to perform accurate and precise Se isotope analysis. If these memory problems could be overcome in the future, the accuracy and precision of Se isotope analysis with n-TIMS can be superior to that achieved with the current HG-ICP-MS technique.

6. Tables and Figures

6.1. Tables

Table 1 – Heat-up sequence for Se isotope analysis on a Triton Plus TIMS

Time [s]	***Aimed filament current [mA]***	***Slope [mA/min]***
0-30	260	520
30-60	456	392
60-90	605	298
90-120	718	226
120-150	802	168
150-180	867	130
180-210	916	98
210-240	953	74
240-270	980	54
270-690	1200	31
690-990	1300	20

Table 2 – The isotope composition of the Se DS

$^{77}Se/^{74}Se$	$^{78}Se/^{74}Se$	$^{80}Se/^{74}Se$
0.6055513	0.0018811	0.0002899

Table 3 - Sequence for measurements at the Thermo Fisher Scientific factory in Bremen

Sequence number	***Sample***
1	SRM 3149 ic
2	SRM 3149 ic
3	$Ba(OH)_2$
4	$Ba(OH)_2$
5	SRM 3149 id
6	DS
7	$Ba(OH)_2$
8	SRM 3149 ic
9	$Ba(OH)_2$
10	$Ba(OH)_2$
11a*and 11b*	SRM 3149 ic
12	SRM 3149 id
13	SRM 3149 id
14*	SRM 3149 ic

*Sequence numbers 11a, 11b, and 14 refer to isotope measurements on the same filament

6.2. Figures

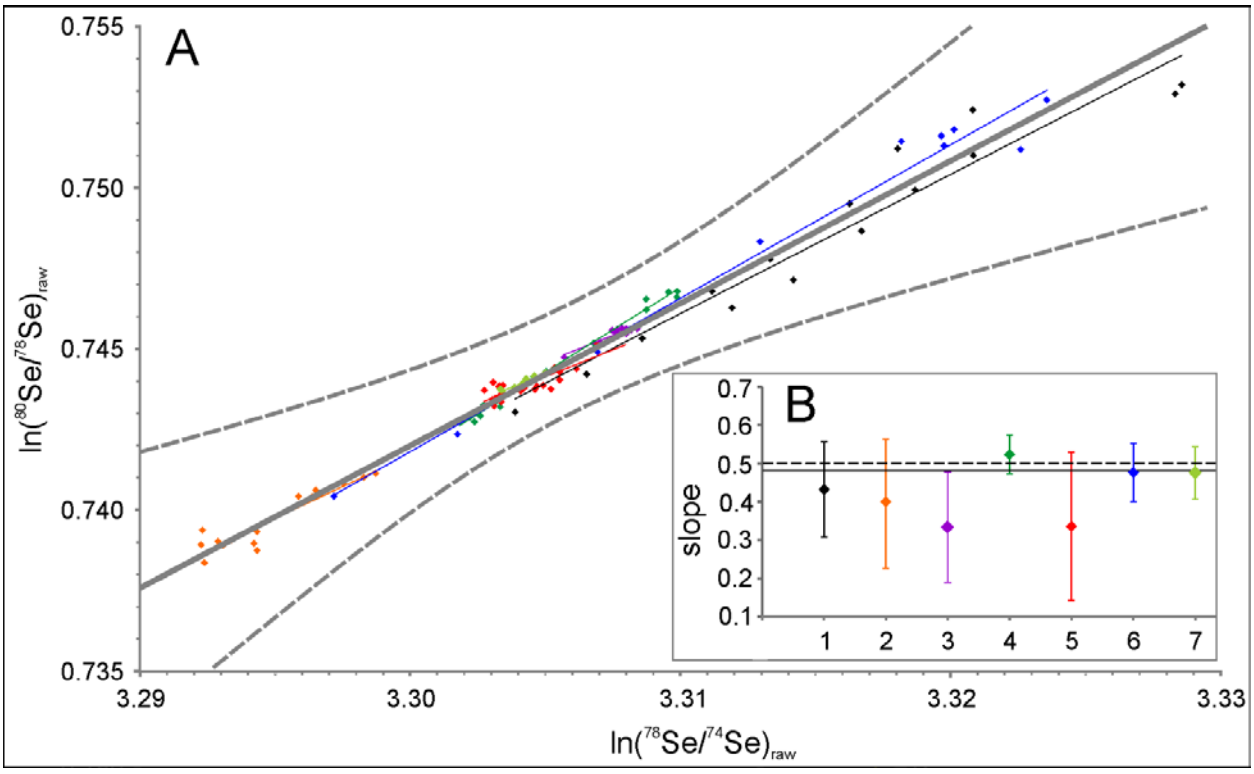

Figure 1 – **A:** Logarithmic raw average $^{80}Se/^{74}Se$ and $^{80}Se/^{78}Se$ ratios of blocks (coloured diamonds, each consisting of 10 cycles) of seven ic SRM 3149 measurements performed in Bern. The measurements were performed before any DS containing standard was introduced to the TIMS. The linear regression through the mean of all blocks defines a slope of 0.441±0.125 (solid grey line with a 2 s.d. (n = 158) uncertainty indicated by dashed grey lines), which overlaps with theoretical predictions from the exponential (0.482) and power (0.500) laws. **B:** The slope of the linear regression through the average ratios of blocks of individual standards (coloured solid lines in **A**) also overlaps within 2 s.d. uncertainty with predictions from power and exponential mass fractionation laws (dashed and solid black horizontal lines, respectively).

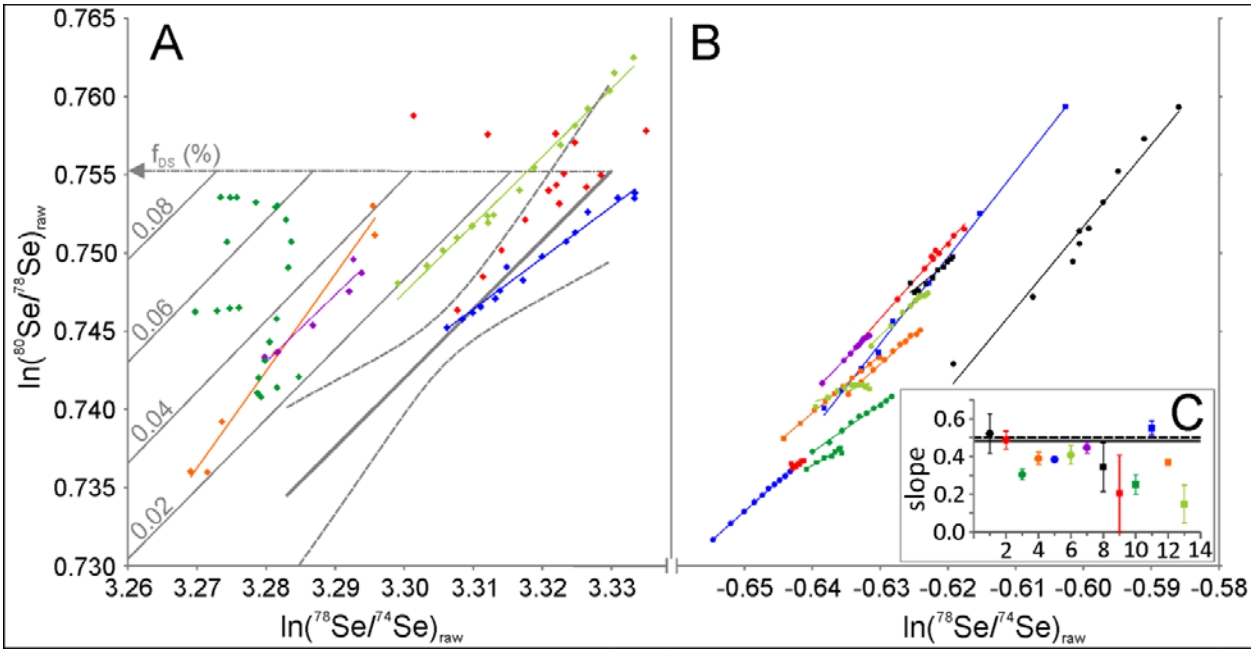

Figure 2 – Logarithmic raw average $^{80}Se/^{74}Se$ and $^{80}Se/^{78}Se$ ratios of blocks (coloured symbols, each consisting of 10 cycles) of later measured ic (**A**) and id (**B**) SRM 3149 measurements performed in Bern. **A:** Solid and dashed thick grey lines represent the linear regression with 2 s.d. from Figure 1. Straight thin grey lines represent calculated mixtures between natural

(represented by the linear regression) and DS Se with numbers indicating the percentage of DS in the mixture. Most of the ic measurements have a different trend than predicted by the mass fractionation laws and are further parallel shifted to the linear regression due to a DS addition of up to 0.08 %. **C:** The slopes of the linear regression through the average id ratios of each block (coloured solid lines in **B)**) do not overlap in most cases within 2 s.d. uncertainty with the predictions from power and exponential mass fractionation laws (dashed and solid grey horizontal lines, respectively).

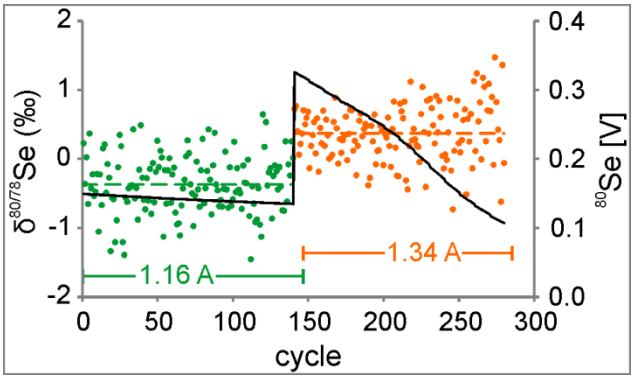

Figure 3 – $\delta^{80/78}$Se and ^{80}Se signal for an id SRM 3149 measurement performed in Bern. Two runs with 14 blocks each consisting of ten cycles and an integration time of 4 s were measured. The first run (green dots with green dashed lined for the average) was measured at 1.16 A filament current, the second run (red dots with red dashed line for the average) was measured at 1.34 A. After the first measurement the filament was heated at a rate of 20 mA/min until the maximum Se signal was reached. The difference in $\delta^{80/78}$Se between the two runs is 0.7‰.

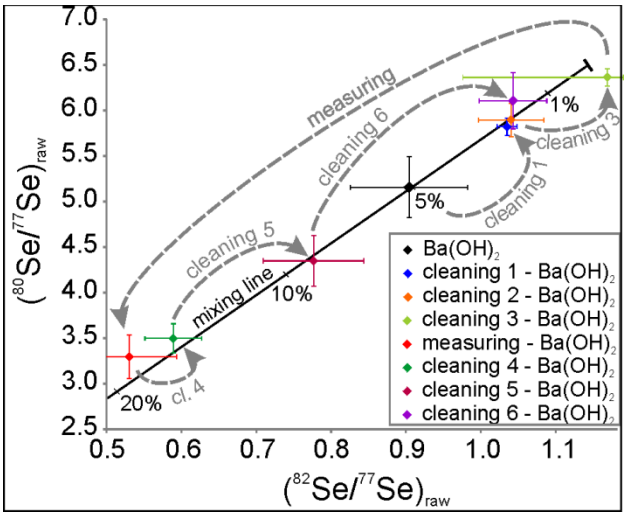

Figure 4 - Effects of cleaning and Se isotope measurements on the Se isotope composition of the memory Se. Each data points represents a measurement of a 1 µl saturated $Ba(OH)_2$ (98 % purity) activator solution after the respective cleaning or measurement step. Straight black line represents the mixing line between Se with natural and spike isotope composition with numbers indicating the amount of DS in the mixture. Cleaning steps: 1. Heating a Re filament at 3 A for 12 h, 2. Cleaning the contact arm, 3. Cleaning the sample chamber and wheel, 4. Heating a Re filament at 5 A for 1 h, 5. Heating a Re filament at 5 A for 3 h, 6. Heating a Re filament at 4 A for 14 h. Between the cleaning steps 3 and 4 two id SRM 3149 standards with 500 ng Se each were measured.

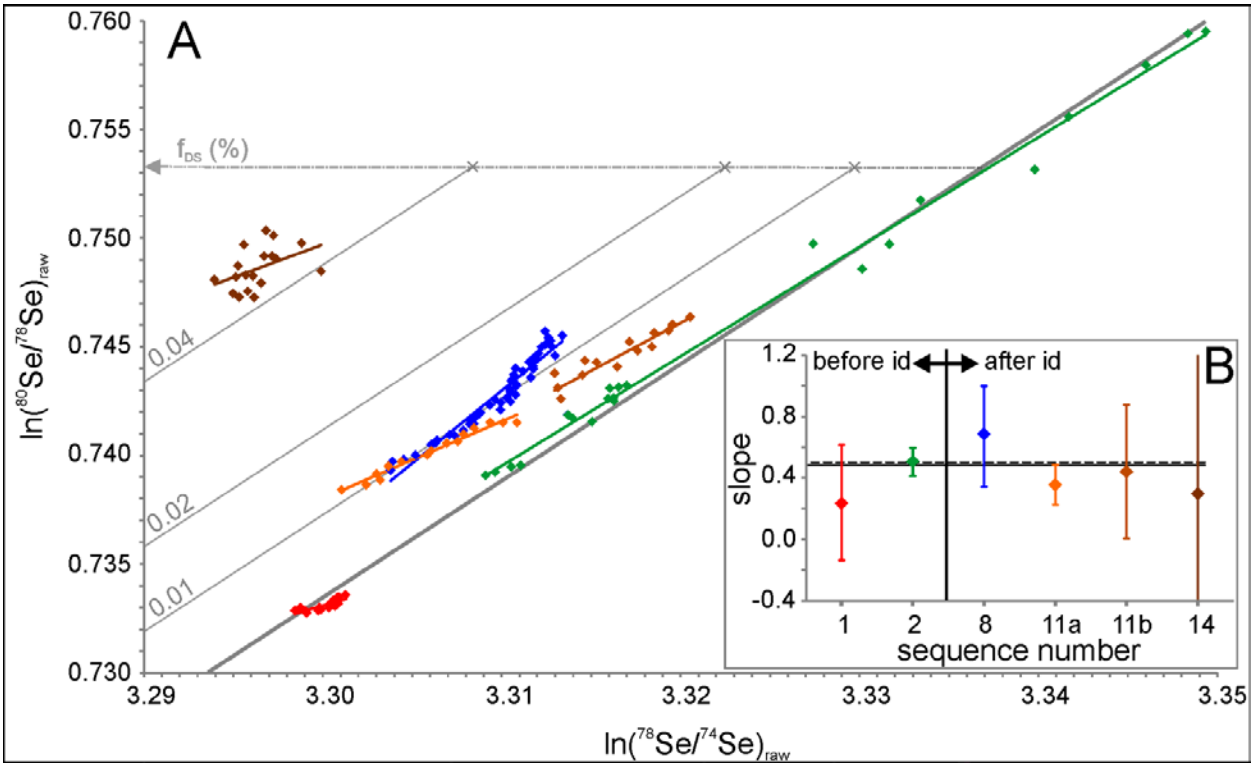

475

476 Figure 5 – **A:** Logarithmic raw average $^{80}Se/^{74}Se$ and $^{80}Se/^{78}Se$ ratios of blocks (coloured
477 diamonds, each consisting of 10 cycles) from ic standards measured at the Thermo Fisher
478 Scientific factory in Bremen. Straight thin grey lines represent calculated mixtures between
479 natural Se and DS with numbers indicating the percentage of DS in the mixture. The linear
480 regression through measured average block ratios of two first measured ic standards (red and
481 green diamonds) defines a slope of 0.537±0.089 (2 s.d., n = 36, thick grey line), which overlaps
482 with predictions from power and exponential mass fractionation laws. Later measured ic
483 standards (blue and orange diamonds), after interim measurements of id standards, are parallel
484 shifted to the linear regression due to the addition of 0.005-0.05 % DS Se. Sequence numbers
485 11a, 11b, and 14 refer to isotope measurements on the same filament (see Table 3) **B:** Despite
486 the shift from the linear regression, the slope of the later measured standards overlap with
487 theoretical estimations from the power (dashed line) and exponential mass fractionation law.

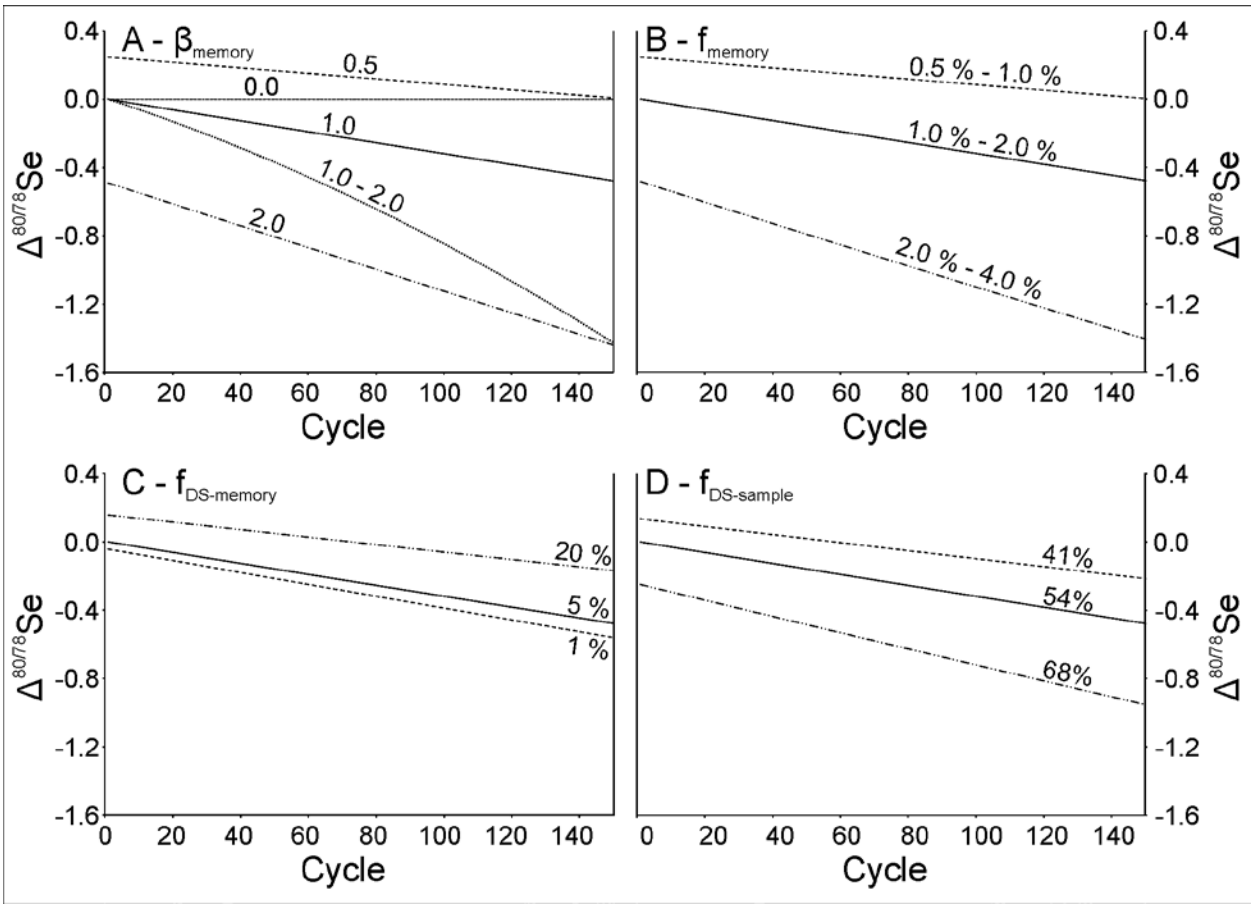

Figure 6 – Results of the model calculations on the impact of DS amount and isotope fractionation of the sample and memory Se on the final $\delta^{80/78}$Se values (see main text for details). The solid black line represents the standard model. **A:** Influence of β_{memory} on the $\Delta^{80/78}$Se of the sample for β_{memory} of 0.0, 0.5, 1.0, 2.0 and a linear increase from 1.0 – 2.0. **B:** Influence of f_{memory} on the $\Delta^{80/78}$Se of the sample for memory fractions of 0.5 % - 1.0 %, 1.0 % - 2.0 %, and 2.0 % - 4.0 %. **C:** Influence of $f_{DS\text{-}memory}$ on the $\Delta^{80/78}$Se of the sample for DS amounts in the memory of 1 %, 5 %, and 20 %. **D:** Influence of $f_{DS\text{-}sample}$ on the $\Delta^{80/78}$Se of the sample for DS amounts in the sample of 41 %, 54 %, and 68 %.

7. Acknowledgements

This research was funded within the framework of the Center for Space and Habitability (CSH) of the University of Bern. We would like to thank G. Baltzer and S. Weissen, T. Johnson, K. Heumann, I. Villa, K. van Zuilen, D. Rufer, and N. Greber for technical assistance and fruitful discussions. The suggestions of two anonymous reviewers greatly helped to improve the manuscript.

8. References

[1] V. Sharma, T. McDonald, M. Sohn, G.K. Anquandah, M. Pettine, R. Zboril, Biogeochemistry of selenium. A review, Environ Chem Lett, 13 (2015) 49-58.

[2] D. Layton-Matthews, M.I. Leybourne, J.M. Peter, S.D. Scott, B. Cousens, B.M. Eglington, Multiple sources of selenium in ancient seafloor hydrothermal systems: Compositional and Se, S, and Pb isotopic evidence from volcanic-hosted and volcanic-sediment-hosted massive sulfide deposits of the Finlayson Lake District, Yukon, Canada, Geochim. Cosmochim. Acta, 117 (2013) 313-331.

[3] K. Mitchell, P.R.D. Mason, P. Van Cappellen, T.M. Johnson, B.C. Gill, J.D. Owens, J. Diaz, E.D. Ingall, G.-J. Reichart, T.W. Lyons, Selenium as paleo-oceanographic proxy: A first assessment, Geochim. Cosmochim. Acta, 89 (2012) 302-317.

[4] P.A.E. Pogge von Strandmann, C.D. Coath, D.C. Catling, S.W. Poulton, T. Elliott, Analysis of mass dependent and mass independent selenium isotope variability in black shales, J. Anal. At. Spectrom., 29 (2014) 1648-1659.

[5] O. Rouxel, Y. Fouquet, J.N. Ludden, Subsurface processes at the lucky strike hydrothermal field, Mid-Atlantic ridge: evidence from sulfur, selenium, and iron isotopes, Geochim. Cosmochim. Acta, 68 (2004) 2295-2311.

[6] H. Wen, J. Carignan, X. Chu, H. Fan, C. Cloquet, J. Huang, Y. Zhang, H. Chang, Selenium isotopes trace anoxic and ferruginous seawater conditions in the Early Cambrian, Chem. Geol., 390 (2014) 164-172.

[7] E.E. Stüeken, J. Foriel, R. Buick, S.D. Schoepfer, Selenium isotope ratios, redox changes and biological productivity across the end-Permian mass extinction, Chem. Geol., 410 (2015) 28-39.

[8] J.-M. Zhu, T.M. Johnson, S.K. Clark, X.-K. Zhu, X.-L. Wang, Selenium redox cycling during weathering of Se-rich shales: A selenium isotope study, Geochim. Cosmochim. Acta, 126 (2014) 228-249.

[9] E.E. Stüeken, R. Buick, A.D. Anbar, Selenium isotopes support free O_2 in the latest Archean, Geology, 43 (2015) 259-262.

[10] S.K. Clark, T.M. Johnson, Selenium Stable Isotope Investigation into Selenium Biogeochemical Cycling in a Lacustrine Environment: Sweitzer Lake, Colorado, J. Environ. Qual., 39 (2010) 2200-2210.

[11] A.S. Ellis, T.M. Johnson, M.J. Herbel, T.D. Bullen, Stable isotope fractionation of selenium by natural microbial consortia, Chem. Geol., 195 (2003) 119-129.

[12] K. Mitchell, R.-M. Couture, T.M. Johnson, P.R.D. Mason, P. Van Cappellen, Selenium sorption and isotope fractionation: Iron(III) oxides versus iron(II) sulfides, Chem. Geol., 342 (2013) 21-28.

[13] T.M. Johnson, M.J. Herbel, T.D. Bullen, P.T. Zawislanski, Selenium isotope ratios as indicators of selenium sources and oxyanion reduction, Geochim. Cosmochim. Acta, 63 (1999) 2775-2783.

[14] J. Far, S. Berail, H. Preud'homme, R. Lobinski, Determination of the selenium isotopic compositions in Se-rich yeast by hydride generation-inductively coupled plasma multicollector mass spectrometry, J. Anal. At. Spectrom., 25 (2010) 1695-1703.

[15] T.M. Johnson, A review of mass-dependent fractionation of selenium isotopes and implications for other heavy stable isotopes, Chem. Geol., 204 (2004) 201-214.

[16] T.M. Johnson, T.D. Bullen, Mass-Dependent Fractionation of Selenium and Chromium Isotopes in Low-Temperature Environments, Reviews in Mineralogy and Geochemistry, 55 (2004) 289-317.

[17] K. Schilling, T.M. Johnson, W. Wilcke, Selenium Partitioning and Stable Isotope Ratios in Urban Topsoils, Soil Sci. Soc. Am. J., 75 (2011) 1354-1364.

[18] E.E. Stueken, J. Foriel, B.K. Nelson, R. Buick, D.C. Catling, Selenium isotope analysis of organic-rich shales: advances in sample preparation and isobaric interference correction, J. Anal. At. Spectrom., 28 (2013) 1734-1749.

[19] J.-M. Zhu, T.M. Johnson, S.K. Clark, X.-K. Zhu, High precision measurement of selenium isotopic composition by hydride generation multiple collector inductively coupled plasma mass spectrometry with a ^{74}Se-^{77}Se double spike, Chinese Journal of Analytical Chemistry, 36 (2008) 1385-1390.

[20] M. Wachsmann, K.G. Heumann, Negative thermal ionization mass spectrometry of main group elements Part 2. 6th group: sulfur, selenium and tellurium, International Journal of Mass Spectrometry and Ion Processes, 114 (1992) 209-220.

[21] A. Krabbenhöft, J. Fietzke, A. Eisenhauer, V. Liebetrau, F. Böhm, H. Vollstaedt, Determination of radiogenic and stable strontium isotope ratios ($^{87}Sr/^{86}Sr$; $\delta^{88/86}Sr$) by thermal ionization mass spectrometry applying an $^{87}Sr/^{84}Sr$ double spike, J. Anal. At. Spectrom., 24 (2009) 1267-1271.

[22] W. Compston, V.M. Oversby, Lead isotopic analysis using a double spike, Journal of geophysical research, 74 (1969) 4338-4348.

[23] J.F. Rudge, B.C. Reynolds, B. Bourdon, The double spike toolbox, Chem. Geol., 265 (2009) 420-431.

[24] T.B. Coplen, J.K. Bohlke, P. De Bievre, T. Ding, N.E. Holden, J.A. Hopple, H.R. Krouse, A. Lamberty, H.S. Peiser, K. Revesz, S.E. Rieder, K.J.R. Rosman, E. Roth, P.D.P. Taylor, R.D. Vocke, Y.K. Xiao, Isotope-abundance variations of selected elements - (IUPAC Technical Report), Pure Appl. Chem., 74 (2002) 1987-2017.

[25] E. Gautier, R. Garavaglia, A. Lobo, M. Fernandez, H. Farach, Isotopic analysis of germanium by thermal ionization mass spectrometry, J. Anal. At. Spectrom., 27 (2012) 881-883.

[26] S.R. Hart, A. Zindler, Isotope fractionation laws: a test using calcium, International Journal of Mass Spectrometry and Ion Processes, 89 (1989) 287-301.

[27] A. Luguet, G.M. Nowell, D.G. Pearson, $^{184}Os/^{188}Os$ and $^{186}Os/^{188}Os$ measurements by Negative Thermal Ionisation Mass Spectrometry (N-TIMS): Effects of interfering element and mass fractionation corrections on data accuracy and precision, Chem. Geol., 248 (2008) 342-362.

[28] M.F. Thirlwall, Long-term reproducibility of multicollector Sr and Nd isotope ratio analysis, Chemical Geology: Isotope Geoscience section, 94 (1991) 85-104.

[29] G. Caro, B. Bourdon, J.-L. Birck, S. Moorbath, ^{146}Sm-^{142}Nd evidence from Isua metamorphosed sediments for early differentiation of the Earth's mantle, Nature, 423 (2003) 428-432.

587 [30] M.O. Naumenko-Dèzes, C. Bouman, T.F. Nägler, K. Mezger, I.M. Villa, TIMS
588 measurements of full range of natural Ca isotopes with internally consistent fractionation
589 correction, Geochim. Cosmochim. Acta, (accepted manuscript).

590 [31] H. Gerstenberger, G. Haase, A highly effective emitter substance for mass spectrometric Pb
591 isotope ratio determinations, Chem. Geol., 136 (1997) 309-312.

592 [32] J.L. Birck, M.R. Barman, F. Capmas, Re-Os Isotopic Measurements at the Femtomole
593 Level in Natural Samples, Geostandards Newsletter, 21 (1997) 19-27.

594 [33] J. Pettersson, A. Olin, The rate of reduction of selenium(VI) to selenium(IV) in
595 hydrochloric-acid, Talanta, 38 (1991) 413-417.

596 [34] A.O. Nier, Variations in the Relative Abundances of the Isotopes of Common Lead from
597 Various Sources, Journal of the American Chemical Society, 60 (1938) 1571-1576.